Asociación Argentina de Astronomía
BAAA, Vol. 50, 2007
G. Dubner, M. Rovira and A. Piatti, eds.

POSTER PAPER

CCD Washington photometry of the moderately metal-poor open cluster NGC 2236

J.J. Clariá[1], A.E. Piatti[2], M.C. Parisi[1], A.V. Ahumada[1]

(1) Observatorio Astronómico de Córdoba, Argentina (OAC)
(2) Instituto de Astronomía y Física del Espacio, Argentina (IAFE)

Abstract. CCD CT_1 Washington photometry in the field of the open cluster NGC 2236 is presented, together with photoelectric CMT_1T_2 photometry of 13 red giant candidates. Based on the best fits of isochrones computed for Z = 0.008 to the (T_1,C-T_1) diagram, we derive reddening, distance and age. A metal abundance [Fe/H] = -0.3 ± 0.2 is estimated from five independent abundance indices. We also derive a cluster core radius of r_c = 1.2 pc and an annular cluster corona of Δr_c = 2.2 pc. The properties of a sample of 20 known open clusters aligned along the line-of-sight to NGC 2236 are examined.

Resumen. Presentamos fotometría de Washington CCD CT_1 en el campo del cúmulo abierto NGC 2236, juntamente con fotometría fotoeléctrica CMT_1T_2 de 13 candidatas a gigantes rojas. En base a ajustes de isócronas teóricas al diagrama (T_1,C-T_1) para Z = 0.008, derivamos enrojecimiento, distancia y edad. La abundancia metálica que resulta a partir de cinco índices de abundancia independientes es [Fe/H] = -0.3 ± 0.2. Se obtienen además valores de 1.2 pc y 2.2 pc para el radio del núcleo y de la corona del cúmulo, respectivamente. Se examinan las propiedades de una muestra de 20 cúmulos conocidos alineados en la dirección de NGC 2236.

1. Structural cluster features

Earlier studies on NGC 2236 prove that there is no agreement on the cluster parameter determination. In fact, the reddening E(B-V) values previously derived range from 0.37 (Phelps et al. 1994) to 0.84 (Babu 1991), while the ages vary from 76 Myr (Babu 1991) to 890 Myr (Janes & Phelps 1994). A redetermination of such parameters is then worth making on the basis of more reliable data.

CCD images of the cluster field were obtained in the Washington C and T_1 bands using the CTIO 0.9 m telescope. These images were reduced using the IRAF package. In addition, 13 red giant candidates were observed photoelectrically with the C, M, T_1 and T_2 filters using the CTIO 1.0 telescope. We applied the method described by Piatti et al. (2005) to estimate a cluster radius of 700 ± 50 pixel, equivalent to 4.7' ± 0.3', and we adopted the region for r > 700 pixel as the "star field area". We also derived a radius r_c = 1.7' at half the maximum

of the cluster density profile, while the cluster corona resulted in an annulus of $\Delta r_c = 1.8\ r_c$. This value does not compare well with the average ratio between the annular width of the corona and the core radius (= 4.3 ± 1.9) found by Nilakshi et al. (2002) for 38 open clusters. A larger sample of star clusters is then required to understand the cause of this disagreement.

2. Cluster fundamental parameters and discussion

We applied the iterative method described by Geisler et al. (1991, hereafter GCM) to derive the cluster metal content. We first assumed that all the red giant candidates are cluster members and we adopted for these stars a wide range of E(B-V) values, varying every E(B-V) 0.05 mag. Once an E(B-V) value was established, we obtained five different values of [Fe/H] from the expression:

$$[Fe/H] = \{-b_i + [b_i^2 - 4a_i(c_i - \Delta_i')]^{1/2}\}/2a_i\,, \qquad (1)$$

where the indices Δ_i' have been defined by GCM and the constants a_i, b_i and c_i are given in GCM's Table 10. The five [Fe/H] values resulting from each adopted reddening were averaged directly to obtain the cluster metal content. This procedure was repeated for different reddening values in order to examine how the metallicity varies as a function of E(B-V). We found that a variation of 0.05 mag in E(B-V) implies a variation of ∼ 0.2 dex in [Fe/H]. We finally adopted E(B-V) = 0.55 for NGC 2236 (see below). The unweighted average of the resulting five [Fe/H] values turned out to be [Fe/H] = -0.30. We then adopted [Fe/H] = -0.3 ± 0.2 for the cluster.

The (T_1,C−T_1) colour-magnitude diagram (CMD) obtained using all the measured stars is depicted in Fig. 1 (left). The well-populated cluster main sequence (MS) is relatively broad, especially in its lower envelope and develops along ∼ 4.5 mag. Fig. 1 (right) shows the (T_1,C-T_1) CMD built using all the measured stars distributed within 700 pixels away from the cluster center. To derive the cluster parameters, we selected three different subsets of isochrones computed by Girardi et al. (2002) for the Washington system - $\log t$ between 8.0 and 9.2 - with Z = 0.008, 0.020 and 0.040, respectively. We independently fitted each isochrone and obtained the corresponding E(C-T_1) colour excess and T_1-M_{T_1} apparent distance modulus. Next, we filled in a grid with four columns containing the assumed Z value, the $\log t$ of the respective selected isochrone, and the E(C-T_1) and T_1-M_{T_1} values obtained for each (Z,$\log t$) pair. Then, we obtained by interpolation the E(B-V) values corresponding to Z = 0.008, 0.020 and 0.040 ([Fe/H] = -0.40, 0.0 and 0.30), respectively, since we have already computed how [Fe/H] varies as a function of E(B-V). Finally, we superimposed the three selected isochrones (one for each Z value) and adopted one of them in turn - the one which best reproduced the cluster MS features and the red giant clump locus - as representative of the cluster age and metal content. Note that isochrones of various metallicities did not yield any negligible differences in the CMD adjustments. The isochrone of $\log t$ = 8.80 (t = 600 Myr) and Z = 0.008 turned out to be the one which most accurately reproduces the cluster features in the CMD. To match this isochrone, we used a E(C-T_1) colour excess and a T_1-M_{T_1} apparent distance modulus of 1.10 and 13.45, respectively. In Fig. 1

(right) we overlapped the zero-age main sequence (ZAMS) and the isochrone of $\log t = 8.80$ (solid lines) for Z = 0.008 on the cluster CMD. The dashed lines correspond to the isochrones of $\log t = 8.70$ and 8.90, which were included for comparison purposes. From the expression E(C-T_1) = 1.97 E(B-V) and M_{T_1} = T_1 + 0.58 E(B-V)-(V-M_V) given by Geisler (1996), we got E(B-V) = 0.55 ± 0.05 and V-M_V = 13.8 ± 0.3. Using A_V/E(B-V)= 3.2, we obtained a true distance modulus V_0-M_V = 12.0 ± 0.4, which implies a distance from the Sun of 2.5 ± 0.5 kpc and a Galactocentric distance of 10.8 kpc, assuming the Sun's distance from the centre of the Galaxy to be 8.5 kpc. Therefore, the position of NGC 2236, its interstellar extinction, its age and its metallicity do seem to be in very good agreement with the generally accepted picture of the structure and chemical evolution of the Galactic disc.

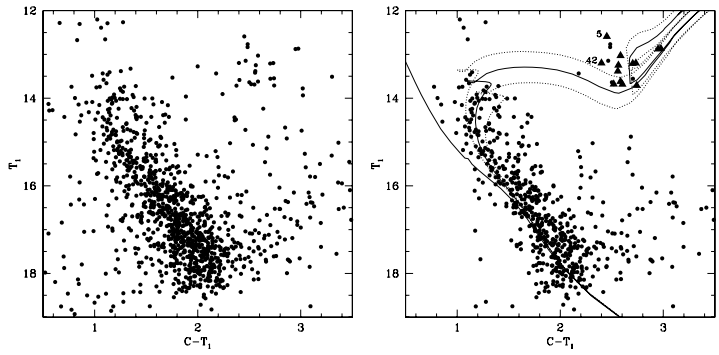

Figure 1. *Left*: (T_1,C-T_1) CMD for stars in the field of NGC 2236. *Right*: r < 700 pixel (T_1,C-T_1) CMD. The ZAMS and the isochrone of $\log t = 8.80$ (Z = 0.008) from Girardi et al. (2002) are overplotted. We marked in dashed lines the isochrones for $\log t = 8.70$ and 8.90. The filled triangles represent the cluster giant candidates photoelectrically observed in the Washington system. Stars 5 and 42 fall slightly outside the range of the GCM's calibration.

The cluster reddening and its distance from the Sun here derived place NGC 2236 among the relatively most reddened and most distant known open clusters projected towards the direction considered, a result which is illustrated in Fig. 2. The upper left hand panel of Fig. 2 shows the distribution of 20 known open clusters projected in the direction $(l, b)_{cluster} = (l, b)_{NGC2236} \pm 5°$. Note that the distance between the outermost and the innermost clusters is nearly 4.7 kpc. The upper right hand panel in Fig. 2 shows the relationship between the visual absorption A_V and the distance d from the Sun. For the sake of comparison, we also included the same relationship corresponding to the Baade's Window - not far from the direction considered here - obtained by Ng et al. (1996), which is represented by a solid line. Note that the Perseus spiral arm - schematically drawn in the figure - causes a large dispersion in the A_V values in the direction considered. Moreover, most of the selected clusters belong to the Galactic plane (see bottom left hand panel), while Berkeley 27 - the furthest and oldest open cluster in the sample (bottom right hand panel) - is only slightly reddened. The Hyades-like age of NGC 2236, its position in the Galactic disc and its metallicity

are consistent with both the existence of a radial abundance gradient ranging from -0.07 to -0.10 dex kpc^{-1} in the Galactic disc and the age-metallicity relation so far delineated by Friel (1995).

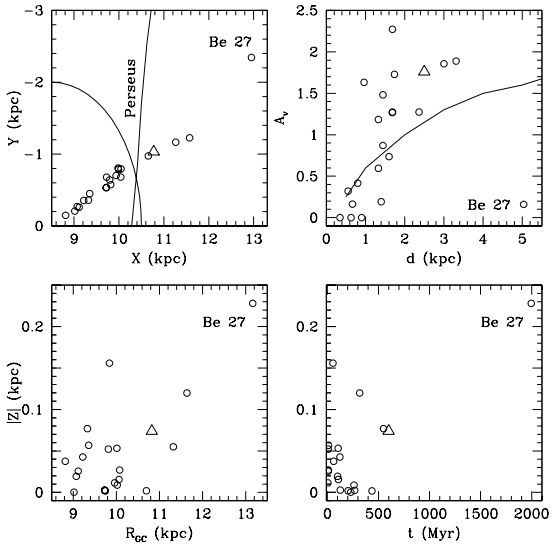

Figure 2. The relationships between the Galactic coordinates X and Y (upper left), between the distance d from the Sun and the visual absorption A_V (upper right), between the Galactocentric distance R_{GC} and the height $|Z|$ out of the Galactic plane (bottom left) and between $|Z|$ and age (bottom right) are presented here for known open clusters projected in the line-of-sight to NGC 2236. Selected clusters and NGC 2236 are indicated by open circles and by an open triangle, respectively. A Sun-centred circle of radius 2 kpc and the Perseus spiral arm are shown in the upper left hand panel. The relationship between d and A_V for Baade's Window is shown in the upper right hand panel.

References

Babu, G.S.D., 1991, JA&A, 12, 187

Friel, E.D., 1995, ARA&A, 33, 81

Geisler, D., 1996, AJ, 111, 480

Geisler, D., Clariá, J.J., Minniti, D., 1991, AJ, 102, 1836 (GCM)

Girardi, L., Bertelli, G., Bressan, A., Chiosi, C., Groenewegen, M.A.T., 2002, A&A, 391, 195

Janes, K.A., Phelps, R.L., 1994, AJ, 108, 1773

Ng, Y.K., Bertelli, G., Chiosi, C., Bressan, A., 1996, A&A, 310, 771

Nilakshi S.R., Pandey, A.K., Mohan, V., 2002, A&A, 383, 153

Phelps, R.L., Janes, K.A., Montgomery, K.A., 1994, AJ, 107, 1079

Piatti, A.E., Clariá, J.J., Ahumada, A.V., 2005, PASP, 117, 22